EFFECT OF THE APPLICATION BETWEEN ANISOTROPIC AND ISOTROPIC DIFFUSE RADIATION MODEL ON BUILDING DIFFUSE RADIATION HEAT GAIN

Zhengrong Li, Haowei Xing*, and Shiqin Zeng
School of Mechanical and Engineering, Tongji University, Shanghai, China

Abstract

The Isotropic Diffuse Radiation Model and Anisotropic Diffuse Radiation Model have been widely applied to building thermal simulation, however, their different performance in simulation have not been fully studied, especially the simulation of building groups. Based on radiation data collected by a radiation station in Shanghai(121.208°E, 31.290°N), an Anisotropic Diffuse Radiation Model(NADR model) and Isotropic Diffuse Radiation Model(IDR model) were used to simulate irradiance values for individual building and building groups, respectively. The analysis results show that diffuse radiation simulation value under the Isotropic Diffuse Radiation Model is relatively small in all orientations for individual building and building groups, except the north. Moreover, the potential impact of applying Isotropic Diffuse Radiation Model on results for thermal simulation and practical application is briefly illustrated.

Keywords: diffuse radiation, anisotropic, radiation model

Introduction

With the urban development and climate change, diffuse radiation value on the facade of buildings is becoming unpredictable, especially for high-rise and high-density buildings. Not only the accurate building energy simulation, but also the design of a future building with very high-energy efficiency demands to study the accurate solar resources in urban environment. Therefore, diffuse radiation models have increasingly become an important part of building thermal environment simulation models.

However, the diffuse radiation model of the existing building thermal environment simulation model, e.g. TUF-3D(Krayenhoff & Voogt, 2007), MUST(X. Yang & Li, 2013), ENVI-met (Kruger, Minella, & Rasia, 2011; Masmoudi & Mazouz, 2004), CTTC(Swaid & Hoffman, 1990), etc. is simplified isotropic diffuse radiation model, while the anisotropic diffuse radiation model is getting developed(Khalil & Shaffie, 2016; Richard Perez, Ineichen, Seals, Michalsky, & Stewart, 1990; D. Yang, 2016).

Furthermore, the research on different performance between isotropic diffuse radiation model and anisotropic diffuse radiation model is limited to individual buildings which are not obstructed, while buildings in complex urban structure are rarely studied. Based on the research on anisotropic sky diffuse radiation model(Richard Perez, Seals, Ineichen, Stewart, & Menicucci, 1987; R. Perez, Stewart, Arbogast, Seals, & Scott, 1986; Yao, Li, Zhao, Lu, & Lu, 2015), this paper will take the buildings in Shanghai, China, as objects to simulate and analyse the effect of these two models on building diffuse irradiance with MATLAB.

Radiation model description

The model in this paper is developed for shortwave radiation heat gain model for buildings. In consideration of anisotropic sky diffuse and complex urban structure, buildings, ground and sky are separated into discrete, 3D element along the x, y and z coordinates. The semi-spherical sky is divided into 8100 pieces every 2 degrees in azimuth and zenith angle, respectively. Next, the calculation of radiation is processed for each element individually.

Anisotropic sky diffuse radiation model

The first diffuse radiation transposition model appeared in the 1960s (Liu & Jordan, 1961). This isotropic diffuse radiation model(IDR model) assumes that the diffuse radiance is uniformly distributed over the sky hemisphere. However, the anisotropic physics of sky radiance has long been demonstrated by Hamilton and Jackson(Hamilton & Jackson, 1985) and others. As a result, an increasing number of sophisticated models have been proposed by treating the sky diffuse component as anisotropic.

Perez(R. Perez et al., 1986) developed a model that attempts to replicate both circumsolar and horizon brightening by superimposing both a disc and a horizontal band with increased radiance upon the isotropic radiance field. The appropriate enhancement factors(F_1, F_2) were evaluated empirically and expressed as a function of the global and direct normal solar irradiances and of the solar zenith angle. Yao(Yao et al., 2015) developed a model(NADR model) based on his measurement in Shanghai(121.51°E,31.28°N) and Perez's method. NADR model adds an orthogonal

diffuse radiation reduction factor(F_3) and corrects enhancement factors(F_1, F_2). In comprehensive consideration of multiple factors such as weather, seasons, orientations, inclination, NADR model is more appropriate and accurate to describe diffuse radiation distribution in Shanghai comparing to Perez model(Yao, Li, Zhao, & Hu, 2014).

The distribution of diffuse radiation on a horizontal surface based on NADR model is shown in Figure 1. Where F_1 is the circumsolar diffuse enhancement factor; F_2 is the horizon diffuse radiation enhancement factors; F_3 is the orthogonal diffuse radiation reduction factor; α is the half angle of the circumsolar zone, set as 10°; ξ is the angular thickness of the horizon band, set as 6.5°; ζ is the half vertex angle of orthogonal zone, set as 17.5°.

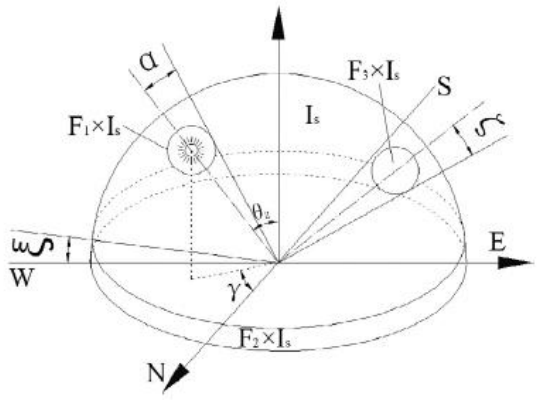

Figure 1: The distribution of diffuse radiation on a horizontal surface in the sky.

Diffuse irradiance calculation

For element i, the diffuse irradiance can be achieved by integrating diffuse radiation from the sky element j. The result is shown as Eq.(1) and be calculated as Eq.(2).

$$I_{dif,i} = \int_{\varphi=0}^{\varphi=2\pi} \int_{\theta=0}^{\theta=\frac{\pi}{2}} I_{\theta,j} sin\theta cos\theta d\vartheta d\varphi \quad (1)$$

$$I_{dif,i} = F_{see} \sum_{j=1}^{8100} I_{\theta,j} cos\theta \frac{S_j}{R^2} \quad (2)$$

where I_i is the diffuse irradiance of element i, W/m^2. $I_{\theta,j}$ is the radiation intensity of sky element j, W/m^2. $F_{see} = \begin{cases} 0, & i \text{ and } j \text{ are visible to each other} \\ 1, & i \text{ and } j \text{ are not visible to each other} \end{cases}$. θ is the incidence angle from j to i, radian. S_j is the area of element j, m^2. R is the radius of sky semi-spherical, m.

Because of the isotropic sky assumption, $I_{\theta,j}$ is equal to each other ($I_{\theta,j} = I_{\theta 0}$). For anisotropic sky model, $I_{\theta,j} = F_j I_{\theta 0}$, where F_j is the correction factor for sky element j, e.g. $F_j = F_1$ for sky elements belong to circumsolar zone.

Global irradiance calculation

Taking multiple reflections among building groups into account, the Gebhart method(Gebhart, 1959) is used to simulate the solar radiation multiple reflections process. The Gebhart absorption factor gives the percentage of energy emitted by a surface that is absorbed by another surface after reaching the absorbing surface by all possible paths. It is obtained by the following

$$G_{ik} = F_{ik}\alpha_i + \sum_{n=1}^{N} F_{in}\rho_n G_{nk} \quad (3)$$

where the factor G_{ik}, G_{nk} is the fraction of energy emitted by *i*, *n* that reaches *k* and is absorbed. F_{ik} is the shape factor of surface element *i* relative to *k*. The surface element number *i* = 1 to *N* and *k* = 1 to *N*. The values of G_{ik}, G_{nk} are different due to different absorptivity ε and albedo ρ, and they are calculated separately.

The global irradiance, $I_{g,i}$, on the surface of element *i* can be calculated as

$$I_{g,i} = I_{dif,i} + I_{dir,i} + I_{ref,i} \quad (4)$$

$$I_{ref,i} = \sum_{k=1}^{N} (I_{dir,k} + I_{dif,k}) \rho_k G_{ki} \quad (5)$$

Where I_{dif} is the diffuse irradiance, W/m^2. I_{dir} is the direct solar irradiance, W/m^2. I_{ref} is the reflected shortwave radiation, W/m^2.

Scenario description

Location description and meteorological data

As typical of the developed cities in China, Shanghai is an appropriate choice to analyse diffuse radiation in building groups. In addition, the research results can be a good reference to other high-rise and high-density cities. The measure data in this paper is collected in Shanghai(121.208°E,31.290°N).

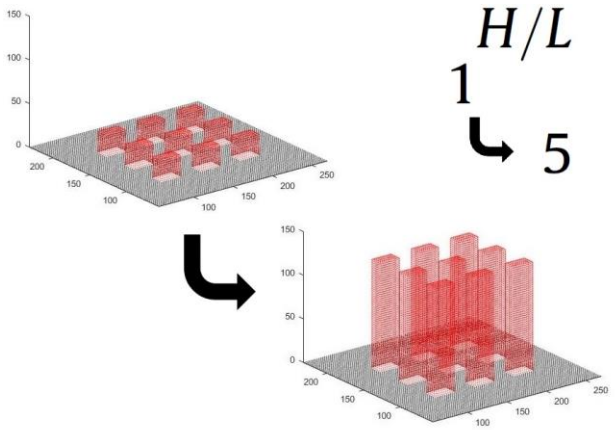

Figure 2: Scenario description of building H/L（1 to 5）.

Parameters description

Effect of the application between anisotropic and isotropic diffuse radiation model is analysed by diffuse irradiance simulation of one individual building and building group. Buildings in this model have a north-south width of 12.5m and east-west length of 25 meters. The height of buildings is represented by H. Albedo(ρ_i) for buildings and ground is 0.4 and 0.2 in shortwave, respectively. Absorptivity(ε_i) equals 1 minus ρ_i. Building groups in this model is formed by 9 individual buildings arranged in 3 rows and 3 columns, as illustrated in figure 2.

Results and discussion

A parametric note: average irradiance in this paper is calculated by averaging simulation value of all elements on one facade. Also, daily irradiance is calculated by averaging simulation value of 24 hours. The default order of four orientations in the following is south-facing, north-facing, west-facing and east-facing.

Individual building

Diffuse and global irradiance on different orientations

Since the average diffuse irradiance of a facade is constant with different ratios of the height to the length (H/L), it is reasonable that analysis of a case with H/L=1 is adequate. The case is processed applying the irradiance data collected on September 24, 2016. Simulation of average diffuse irradiance on different orientations with two models are shown in Figure 3-6.

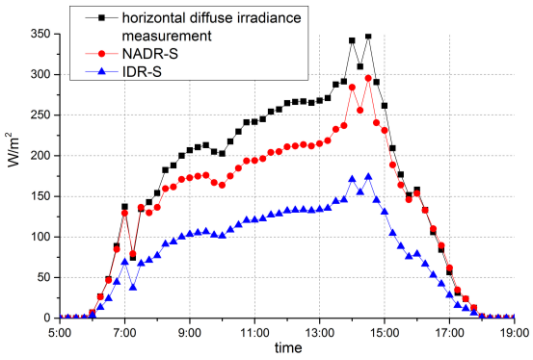

Figure 3: Simulation of average diffuse radiation on south-facing facade of an individual building.

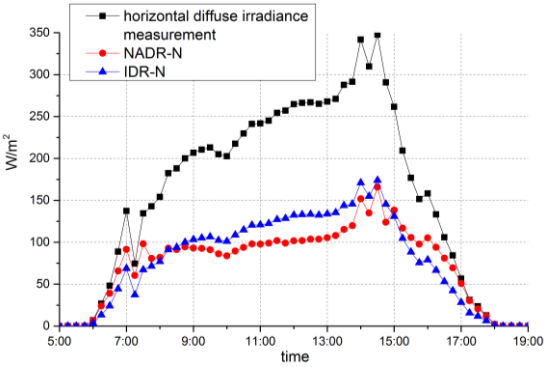

Figure 4: Simulation of average diffuse radiation on north-facing facade of an individual building.

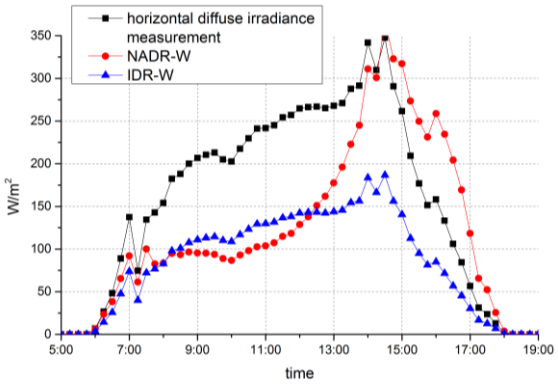

Figure 5: Simulation of average diffuse radiation on west-facing facade of an individual building.

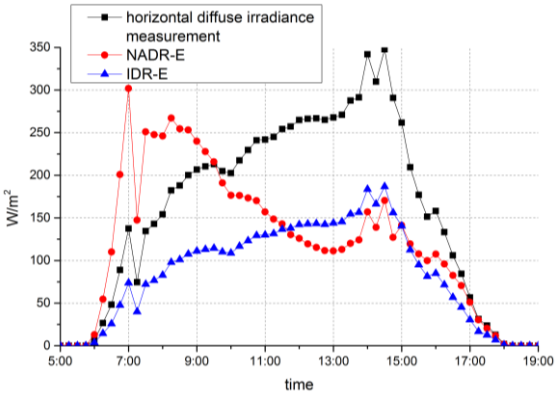

Figure 6: Simulation of average diffuse radiation on east-facing facade of an individual building.

Figure 3-6 show that average diffuse irradiance on facades of different orientations with IDR model are identical and equal to half of the horizontal diffuse irradiance because of the isotropic sky assumption. For NADR model, average diffuse irradiance on facades of different orientations varies with the changes of solar position. The largest average diffuse irradiance occurs on east-facing facade in the morning and moves to south-facing, west-facing facade when it comes to noon and afternoon respectively. However, average diffuse irradiance on north-facing facade performs smaller comparing to those of other orientations at most moment. Judging from the daily irradiance on four different orientations, south-facing facade receives the most diffuse irradiance and north-facing one receives the least, while east-facing and west-facing facade ranks the same. The reason for this phenomenon is the circumsolar diffuse radiation which follows the sun's trajectory.

Based on the statistical data, ratio of daily diffuse irradiance on four orientations to daily horizontal diffuse irradiance is 0.8518, 0.4797, 0.7745, 0.7757 with NADR model and 0.4999, 0. 4999, 0.4999, 0.4999 with IDR model. The relative difference of average diffuse irradiance on four orientations is +41.33%, -4.22%, +30.66%, +30.75% with two models.

Global irradiance is calculated as Eq.(4) and the result comes out similar to diffuse irradiance, i.e., simulation

value of global irradiance on façades exposed to sun with NADR model is larger than that with IDR model as a result of circumsolar diffuse radiation. The relative difference of average global irradiance on four orientations is +17.03%, -5.55%, +15.84%, +13.52%.

Irradiance under different solar position

Considering that the irradiance is strongly correlated with sun position and the simulation in 4.1.1 is unrepresentative throughout a year, simulation date is set on March 20, June 21 and December 21 to study irradiance on façade of different orientations during an entire year.

Result of simulation with two models shows the relative difference of average diffuse irradiance on four orientations is +38.32%, -5.13%, +29.92%, +29.83% at the vernal equinox, which is similar to the result in 4.1.1. The difference at the summer solstice and winter solstice is 0.80%, -2.17%, +18.73%, +17.35% and +63.12%, +9.88%, +39.04%, +40.11%, respectively. It can be seen from the simulation value that difference between NADR model and IDR model increases with an increment of solar zenith angle. Additionally, south-facing facades are the most sensitive to solar zenith angle among four orientations and north-facing is the least sensitive one, while west-facing façade and east-facing façade perform similarly medium.

Building groups

Diffuse irradiance on different orientations

Since the building groups in this model is formed by 9 individual buildings arranged in 3 rows and 3 columns, 5# building which is located in the centre of 9 buildings is studied as a typical building in complex urban structure.

Statistics shows that the effect of the application between two models on building radiation simulation is similar to the result in 3.1, i.e., NADR model performs larger on all orientations except northern. The amount of diffuse irradiance throughout the day is added and shown in Figure 7.

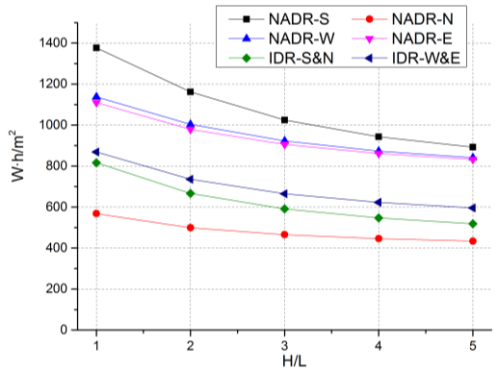

Figure 7: Simulation of diffuse irradiance throughout the day on four facades of 5# in building groups with different H/L.

Furthermore, the ratio of simulation value with NADR model to that with IDR model is presented in Figure 8. As the figure shows, difference between two models on south-facing façade stays essentially unchanged with the increase of H/L, while the difference increases on west-facing(+10.3%), east-facing(+12.1%) façade and decreases on north-facing façade(-14.1%), respectively. This result means simulation with IDR model tends to underestimate more diffuse irradiance in high-rise and high-density buildings comparing to common low-rise and low-density buildings, especially on west-facing and east-facing facades.

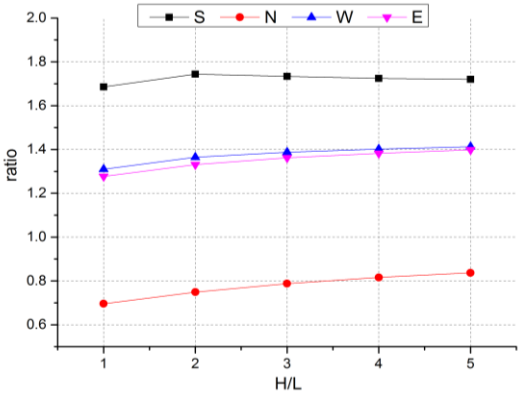

Figure 8: ratio of simulation value with NADR model to that with IDR model on four facades of 5# in building groups with different H/L.

In order to study the effect of the application between two models on diffuse radiation at different moment throughout the day, average diffuse irradiance on west-facing of 5# is divided by that of individual building in 4.1, the ratio is shown in Figure 9,10.

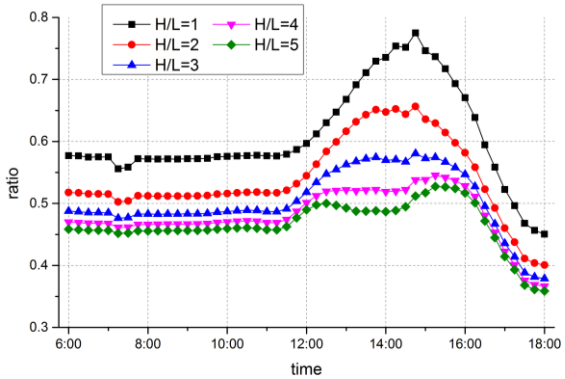

Figure 9: ratio of average diffuse radiation on west-facing facade of 5# in building groups with different H/L (NADR model).

Figure 9 illustrates that average diffuse irradiance with NADR model on west-facing façade decreases with the increase of H/L. However, the reduction proportion

varies at different moment throughout the day. Average diffuse irradiance on west-facing façade decreases more rapidly in the afternoon comparing to other moments throughout the day, which reflects the impact of circumsolar diffuse radiation and obstructing between buildings. For IDR model, the percentage of reduction is equal, as shown in Figure 10. The comparison of two models has a similar trend on the other three orientations.

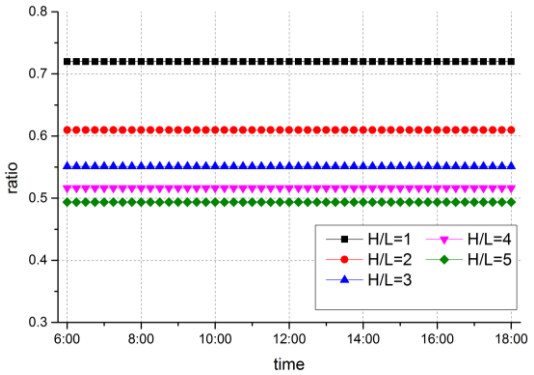

Figure 10: ratio of average diffuse radiation on west-facing facade of 5# in building groups with different H/L (IDR model).

Vertical stratification of diffuse irradiance on four orientations

An general parameter (average diffuse irradiance) may not be enough to describe the distribution of diffuse radiation on a facade, especially for high-rise and high-density buildings(irradiance is quite different between the top and the bottom of a building). To research on the vertical stratification of diffuse irradiance on a façade, diffuse irradiance on south-facing façade of #5 is plotted every 6.25m in Figure 11.

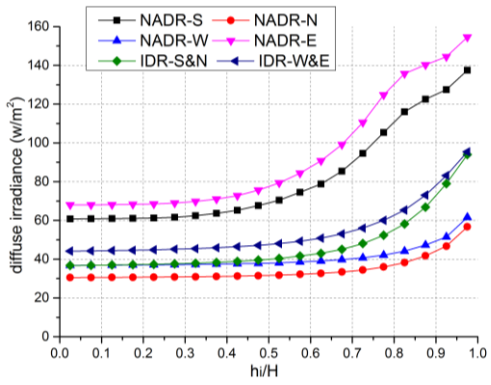

11: Vertical stratification of diffuse irradiance on four façades of 5# applying two models （H/L=5）.

The curves derived from the IDR model in Fig.10 depicts that façades of equal sky view factor have the same characteristics, such as the south-facing facade and the north-facing façade. Specifically, the diffuse irradiance that one point receives increases with the increase of sky view factor and thus with the increase of height. However, the curves derived from the NADR model reveals more details closer to the physics. NADR model illustrates that vertical stratification of diffuse irradiance has a little difference when h/H is lower than 3/5, while increase gradient becomes large above 3/5 of the height. The above phenomenon can be explained by a coupling influencing of circumsolar diffuse radiation and the obstructed irradiance on the bottom half of buildings caused by other buildings. This phenomenon is drawn in Figure 12

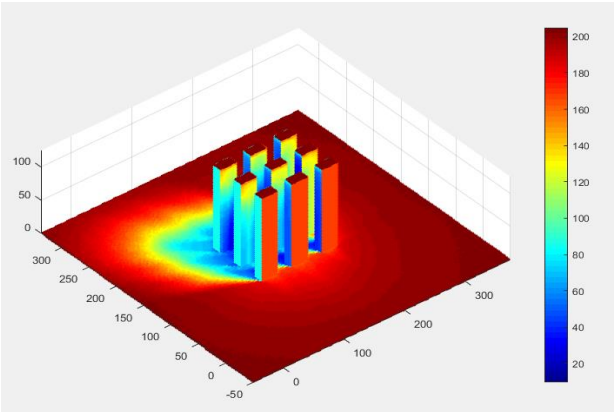

Figure 12: Simulation of diffuse radiation on a building group at 10:00am on September 24, 2016 in Shanghai.

To sum up, there are significant differences in diffuse irradiance distribution on facades comparing two models. Furthermore, deviation of the two models increases with the increment of H/L.

Sky diffuse model validation

The validation of NADR model has been completed by Yao(Yao et al., 2015), however, measure data collected between September 2016 to November is analysed to verify the accuracy of NADR model. In considering that it is appropriate and common to use R.S.D.(relative standard deviation) error values to describe the deviation between two model performances, results below are presented with R.S.D.. R.S.D. error of NADR and IDR model is 18.66%, 36.07% respectively on non-overcast condition and 46.64%, 22.73% respectively on overcast condition. The statistics illustrates that NADR model performs better than the IDR model for non-overcast skies, but an inferior accuracy on an overcast day. Thus, the NADR model should be applied unless it is completely overcast sky.

Nevertheless, the inferior accuracy on an overcast day is not the problem of anisotropic diffuse radiation model itself, but the limitation of NADR model. With the development of anisotropic diffuse radiation model, there will be a satisfactory performance for anisotropic diffuse radiation model on an overcast day.

Conclusion

Based on the measure data collected in Shanghai(121.208°E,31.290°N), one individual building and building groups with different values of the H/L is stimulated by applying Anisotropic Diffuse Radiation Model (NADR model) and Isotropic Diffuse Radiation Model (IDR model). Several conclusions can be drawn as below:

1. Diffuse irradiance on façade of individual buildings with isotropic model is generally lower comparing to that with anisotropic model, the deviation on four orientations(SNWE) is +41.33%, -4.22%, +30.66%, +30.75%, respectively. Additionally, the deviation increases with the increment of solar zenith angle, which suggests the temperature of a façade exposed to solar beam and cooling load will be underestimated when applying isotropic model, especially in the afternoon for the Northern Hemisphere. This conclusion requires significant attention at the stage of design and operation of buildings
2. The effect of application between two models on building groups is similar to individual buildings, and the deviation rises with the increment of H/L for all orientations except the north.
3. As far as one point on a façade of building located in building groups is concerned, irradiance and its increase gradient enhances with the elevation of height. According to the analysis, anisotropic model performs more accurate than isotropic model by reflecting the realistic impact of circumsolar diffuse.

with the rapid urbanization, research on accurate solar resources is required for not only average irradiance on a façade, buy also the distribution on a façade, especially in high-rise and high-density building groups.

Since the current common isotropic sky model is not perfect enough to simulation irradiance, the anisotropic sky model should be proposed to prevent thermal energy simulation errors in the design stage of buildings and do contribution to building energy efficiency. Besides, the simulation on an overcast day with anisotropic model will be modified with the improvement of models.

Nomenclature

F_1 circumsolar diffuse enhancement factor

F_2 horizon diffuse radiation enhancement factors

F_3 orthogonal diffuse radiation reduction factor

F_j correction factor for sky element j

F_{see} visible factor

F_{ik} shape factor

G_{ik} Gebhart absorption factor

H height of a point on the building

H height of a building

i element of buildings and ground

I_{dif} diffuse irradiance (W/m^2)

I_{dir} direct solar irradiance (W/m^2)

I_g global irradiance (W/m^2)

I_{ref} reflected shortwave radiation (W/m^2)

$I_{\theta 0}$ radiation intensity of isotropic sky (W/m^2)

$I_{\theta,j}$ radiation intensity of sky element j (W/m^2)

j element of sky

k element of buildings and ground

L length of a building

n element of buildings and ground

R the radius of sky model (m)

S_j the area of element j (m^2)

W width of a building

Greek symbols

α half angle of the circumsolar zone (degree)

ε absorptivity

ζ half vertex angle of orthogonal zone (degree)

θ the incidence angle form j to i (rad)

ξ angular thickness of the horizon band (degree)

ρ albedo

References

Gebhart, B. (1959). A New Method for Calculating Radiant Exchanges. *ASHRAE Trans., 65*(1), 321-332

Hamilton, H. L., & Jackson, A. (1985). A shield for obtaining diffuse sky radiation from portions of the sky. *Solar Energy, 34*(1), 121-123

Khalil, S. A., & Shaffie, A. M. (2016). Evaluation of transposition models of solar irradiance over Egypt. *Renewable and Sustainable Energy Reviews, 66*, 105-119

Krayenhoff, E. S., & Voogt, J. A. (2007). A microscale three-dimensional urban energy balance model for studying surface temperatures. *Boundary-Layer Meteorology, 123*(3), 433-461

Kruger, E. L., Minella, F. O., & Rasia, F. (2011). Impact of urban geometry on outdoor thermal comfort and air quality from field measurements in Curitiba, Brazil. *Building and Environment, 46*(3), 621-634

Liu, B. Y. H., & Jordan, R. C. (1961). Daily insolation on surfaces tilted towards equator. *ASHRAE Trans., 10*, 53-59

Masmoudi, S., & Mazouz, S. (2004). *Relation of geometry, vegetation and thermal comfort around buildings in urban settings, the case of hot arid regions*.

Perez, R., Ineichen, P., Seals, R., Michalsky, J., & Stewart, R. (1990). Modeling daylight availability and irradiance components from direct and global irradiance. *Solar Energy, 44*(5), 271-289

Perez, R., Seals, R., Ineichen, P., Stewart, R., & Menicucci, D. (1987). A new simplified version of the perez diffuse irradiance model for tilted surfaces. *Solar Energy, 39*(3), 221-231

Perez, R., Stewart, R., Arbogast, C., Seals, R., & Scott, J. (1986). An anisotropic hourly diffuse radiation model for sloping surfaces: Description, performance validation, site dependency evaluation. *Solar Energy, 36*(6), 481-497

Swaid, H., & Hoffman, M. E. (1990). Prediction of urban air temperature variations using the analytical CTTC model. *Energy and Buildings, 14*(4), 313-324

Yang, D. (2016). Solar radiation on inclined surfaces: Corrections and benchmarks. *Solar Energy, 136*, 288-302

Yang, X., & Li, Y. (2013). Development of a Three-Dimensional Urban Energy Model for Predicting and Understanding Surface Temperature Distribution. *Boundary-Layer Meteorology, 149*(2), 303-321

Yao, W., Li, Z., Zhao, Q., & Hu, L. (2014). Comparative study on accuracy of several diffuse radiation models. *Journal of Tongji University, 42*(6), 937-943

Yao, W., Li, Z., Zhao, Q., Lu, Y., & Lu, R. (2015). A new anisotropic diffuse radiation model. *Energy Conversion and Management, 95*, 304-313